The effect of pacing pellets on ELMs, W impurity behaviour and pedestal characteristics in high-power, JET-ILW H-mode plasmas

A. R. Field[1], P. Carvalho[2], L. Garzotti[1], H-T. Kim[3], M. Lenholm[1,3], E. Lerche[1,4], C. Maggi[1], A. Meigs[1], F. Rimini[1], C. Roach[1], S. Saarelma[1], M. Sertoli[1,5] and JET contributors*

EUROfusion Consortium, JET, Culham Science Centre, Abingdon, OX14 3DB, UK

[1]CCFE, Culham Science Centre, Abingdon, OX14 3DB, UK

[2]IPFN, Instituto Superior Técnico, Universidade de Lisboa, 1049-001 Lisboa, Portugal

[3]EUROfusion Programme Management Unit, Culham Science Centre, Abingdon, OX14 3DB, UK

[4]LPP-ERM-KMS, Association EUROFUSION-Belgian State, TEC partner, Brussels, Belgium

[5]Max-Planck-Institut für Plasmaphysik, Boltzmannstrasse 2, D-85748 Garching, Germany

**see the author list of E. Joffrin et al., 27th IAEA FEC Ahmedabad, India 2108, submitted to N. Fus.*

In high-performance, ITER baseline-scenario pulses (3MA/2.7T) in JET-ILW with high levels (~ 32 MW) of heating power, typically ~ 20-40% of the input power is radiated, predominantly by W impurities, which are sputtered from the divertor targets and reach the confined plasma. Sustained ELMy H-mode operation at such heating powers in JET-ILW requires gas puffing to increase the ELM frequency and hence the rate of W flushing from the confined plasma, as well as strike point sweeping to avoid overheating of the target material [1]. Core ICRH heating is also used for control of heavy impurity accumulation. A deleterious effect of the gas puffing is to reduce the pedestal temperature [2] by increasing the pedestal heat transport between ELMs [3, 4], which reduces the pedestal pressure [5] and the overall confinement compared to that achieved in similar JET-C pulses at the same heating power without sustained gas puffing.

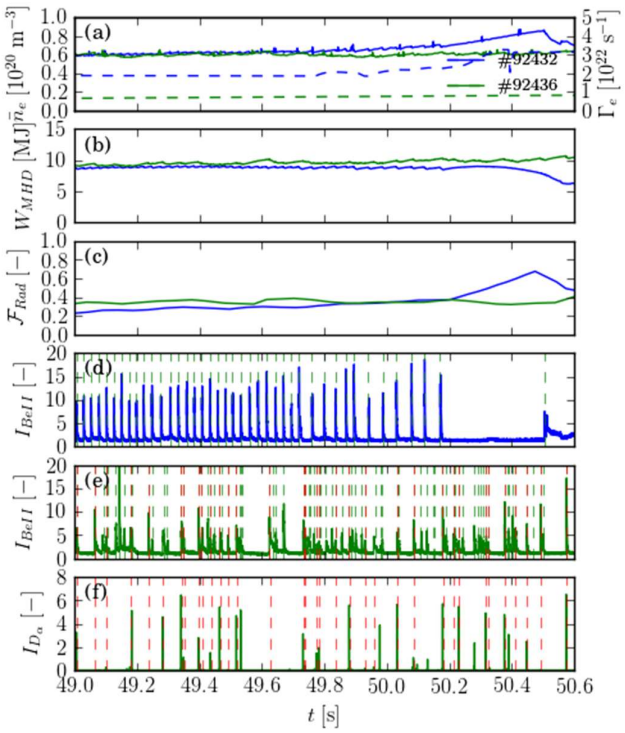

Fig. 1 Comparison for pulses #92432 (gas only) and #92436 (pellets & gas) of: (a) line-average density $\bar{n}_e$ and gas fuelling rate Γ_D (dashed), (b) stored energy W_{MHD}, (c) radiated power fraction $\mathcal{F}_{rad}$, (d, e) Be II intensity viewing divertor I_{BeII}, and (f) D_α intensity viewing the pellet entry.

With gas fuelling alone, if the puffing rate is insufficient, the duration of high-power JET-ILW baseline pulses can be limited by a gradual increase of the W content and associated radiation, e.g. as occurs in the gas-fuelled pulse #92432 shown in Fig. 1. This reduces the ELM frequency, further increasing the radiation and eventually triggers a transition to L-mode, after which the W accumulates in the core, thereby ending the high-performance phase.

Partially replacing some (~ 30%) of the gas puffing by injection of small, ELM-pacing pellets, resulting in ~ 30% less fuelling overall, is found both to extend duration of the ELMy H-mode phase and to enhance the overall confinement compared to that achieved with gas fuelling alone. As shown in Fig. 1 (e, f), the pacing pellets induce more frequent, irregular ELMs of smaller amplitude than those occurring naturally with gas fuelling.

Another beneficial effect of operating at a reduced gas puffing rate with

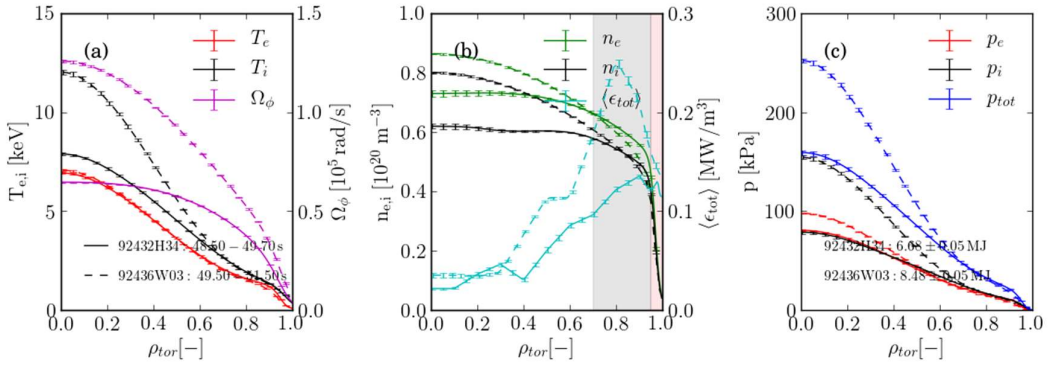

Fig. 2 Comparison of fitted, time-averaged kinetic profiles for pulses #92432 (gas only) and #92436 (pellet & gas) showing radial profiles of: (a) ion and electron temperatures $T_{i,e}$ and toroidal rotation rate Ω_ϕ; (b) ion and electron densities $n_{i,e}$ and flux-surface averaged total emissivity $\langle\varepsilon_{tot}\rangle$; and (c) ion, electron $p_{i,e}$ and total p_{tot} pressures. The averaging times are: 48.5-50.0s for #92432 and 49.5-51.5 s for #92436.

pacing pellets is an enhancement of the core energy confinement, which is associated with increased toroidal rotation and reduced ion temperature gradient stiffness [8]. A comparison of kinetic profiles of gas-only pulse #92432 and pulse #92436 with pellets and gas puff is shown in Fig. 2, from which it can be seen that pulse #92436 has higher (≤ ×1.7) rotation rate Ω_ϕ, and hence E×B shear Γ_E. This reduces the ion heat diffusivity χ_i by a factor ≤ 5 compared to that in #92432 and to within a factor ≥ 3 of the neo-classical value $\chi_{i,NC}$. The resulting increased ion pressure p_i results in ~ 20% more stored thermal energy than in the gas-only pulse #92432.

In such high-power pulses, the radiation is dominated by W impurities, predominantly from the outer, 'mantle' region ($0.7 \leq \rho \leq \rho_{ped} \sim 0.96$), where they can be efficiently flushed by ELMs. A measurement of the W flushing efficiency of each ELM $\Delta\bar{n}_Z/\bar{n}_Z$ (here Z refers to W as the dominant high-Z impurity) can be evaluated from fast bolometric measurements of the radiated power P_{Rad}^{TOBH} and the line-average density $\bar{n}_e$ from the lower, horizontal interferometer channel (#5) by availing of fact that the total emission rate coefficient ξ_W of W over the 1-2 keV temperature range in the mantle region is almost constant $\bar{\xi}_W \sim 4.5\times10^{-31}$ Wm^3, i.e. by assuming $\Delta\bar{n}_Z \propto \Delta(P_{Rad}^{TOBH}/\bar{n}_e)$ [6]. This and a similar measure estimating the W ingress (fluence) between ELMs can be used to calculate the net rate of change of the impurity content, $\Upsilon_Z = (d\bar{n}_Z/dt)/\bar{n}_Z$. Fig 3 (b, c) shows $\Delta\bar{n}_Z/\bar{n}_Z$ and rates Υ_Z due to the ELM flushing, inter-ELM fluence and the 'net' change due to the balance between these competing fluences, i.e. $(\Delta\bar{n}_Z/\bar{n}_Z)_{net} = (\Delta\bar{n}_Z/\bar{n}_Z)_{ELM} - (\Delta\bar{n}_Z/\bar{n}_Z)_{i-ELM}$ and $\Upsilon_{Z,net} = \Upsilon_{Z,ELM} - \Upsilon_{Z,i-ELM}$. In the case of a group of rapid ELMs, with an inter-ELM period shorter than the pre-/post-ELM averaging times {-7, 10 ms}, it is only possible to determine the flushing for the group, which is split equally between the sub-ELMs, while the inter-ELM fluence is allocated to the last in the group. A property of this ad-hoc method of handling the compound ELMs does maintain valid, time-averaged flushing rates Υ_Z calculated from the $\Delta\bar{n}_Z/\bar{n}_Z$ data.

In pulse #92432, each ELM flushes ~ 5-10% of the W content (mean concentration $\bar{C}_W \sim 2\times10^{-4}$) and a similar amount enters the plasma between the ELMs, resulting in a gradual net increase over a timescale $1/\Upsilon_W \sim$ few seconds. During the sustained ELMy H-mode phase, outward neo-classical convection in the mantle, which is proportional to the parameter $\zeta_{NC} = R/2L_{T_i} - R/L_{n_i}$ [7], helps concentrate the W in this region (see Fig. 3 (d, e)). However, after the transition to L-mode, ζ_{NC} decreases sharply to ~ 0 and the W accumulates in the core.

In contrast, pulse #92436 with ELM pacing pellets, has smaller, irregular ELMs, which are sustained, maintaining a slightly higher $\bar{C}_W \sim 2.5\times10^{-4}$. Although ζ_{NC} is sometimes small, allowing some ingress of W deeper into the plasma, there is no strong accumulation as in the

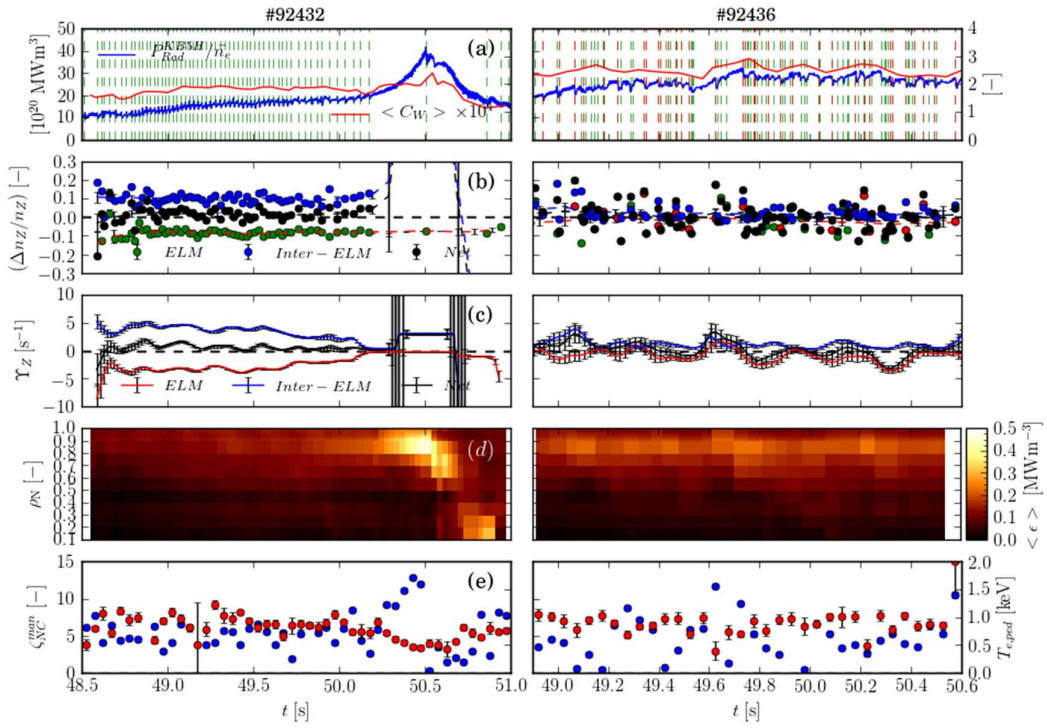

Fig. 3 Comparison for pulses #92432 (left, gas only) and #92436 (right, pellets & gas) of: (a) the signal $P_{Rad}^{TOBH}/\bar{n}_e$ (blue) and average W concentration $\bar{C}_W$ (red); (b) relative change in W content $\Delta n_W/n_W$ due to ELMs (natural-●, pellet-●), inter-ELM fluence (●) and net change per-ELM (●); (c) the associated rates of change Υ_Z; (d) flux-surface averaged emissivity $\langle\varepsilon_{tot}\rangle$ vs ρ_{tor}; and (e) the N-C convection parameter ζ_{NC} averaged over the mantle (●) and pedestal temperature $T_{e,ped}$ (●).

L-mode phase of #92432. With the higher frequency, irregular ELMs, there is much greater variation in the ELM flushing and inter-ELM fluence data than in the gas-only pulse #92432.

By classifying ELMs as either 'pellet-triggered' or 'natural' events, the $\Delta\bar{n}_Z/\bar{n}_Z$ data can be conditionally averaged, thereby quantifying the data according to ELM type. Fig 4 (a, b) shows such data for four high-power 3 MA pulses: #92432:3 with gas fuelling (2.2:2.6×10^{22} e/s) and #92434:6 with both gas fuelling (0.6:0.8×10^{22} e/s) and pellets. Also shown in Fig 4 (c, d) are relative, intra-ELM Be and W fluences $\Phi_{Be,W}$ estimated (assuming constant ionisations/photon S/XB) from time-integrated Be II (527 nm) and W I (401 nm) line intensities from a multi-chord spectrometer viewing the outer divertor targets. The bremsstrahlung contribution to the WI line (detected by a LoS viewing through the x-point) is estimated to be ≤ 10% during ELMs.

Conditionally averaged values of the data shown in Fig. 4 according to ELM type are given in Table 1. The amplitude, expressed in terms of $\Delta\bar{n}_e/\bar{n}_e$, of the 'pellet-triggered' ELMs is about half of that of the natural ELMs. For the gas-fuelled pulses, the W flushing efficiency of the 'natural' ELMs is ~ 5 times that of that for both ELM types in the pellet fuelled pulses. The inter-ELM W fluences are also smaller in the pellet-fuelled pulses, partly due to the shorter inter-ELM periods. In the case of the inter-ELM fluences, it is more meaningful to compare the rate $\Upsilon_{Z,i-ELM}$ shown in Fig. 3 (c), which is in any case smaller in the pulse #92436 with pellets than in the gas-only pulse #92432, however, the resulting net rate of change $\Upsilon_{Z,net}$ is similar.

Mean values of ζ_{NC} across the pedestal and mantle regions, averaged over Δt_{ELM} ≤ 20 ms (evaluated from fits to high-resolution Thomson scattering T_e and n_e profile measurements, assuming $T_i = T_e$) for the different cases are also given in Table 1, classified according to the preceding ELM type. In the pellet-fuelled pulses, after the natural ELMs, ζ_{NC} in the mantle

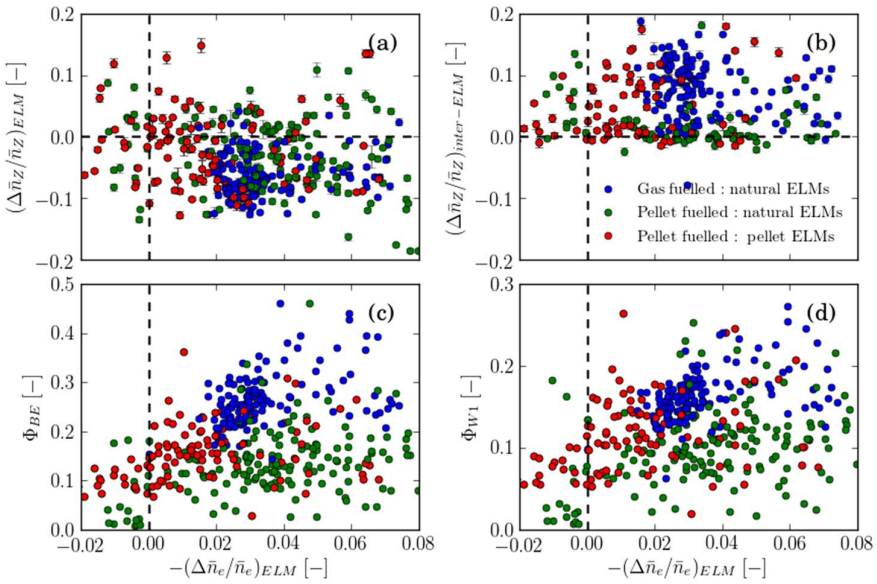

Fig. 4: Comparison of data from high-power 3 MA/2.7T pulses with only gas (● #92432/3) and with pellet & gas fuelling (●/● #92434/6) for pellet triggered (●) and natural (●/●) ELMs showing: the relative change in W content $\Delta n_W/n_W$ due to ELMs (a) and inter-ELM fluence (b); (c, d) relative intra-ELM fluences $\Phi_{Be/W}$ of Be and W impurities from visible-range divertor spectroscopy.

region is significantly lower (~ ×0.6) than after those in the gas-only pulses, which have ~ 3 times higher D_2 puffing rate, while ζ_{NC} is lower (~ ×0.7) in the pedestal region after the pellets. The relative, intra-ELM impurity fluence data shown in Fig. 4 (c, d), reveals that the intra-ELM Be and W fluences $\Phi_{Be,W}$ are on average larger (by factors ~ 1.8 and ~ 1.4) for the ELMs in the gas-fuelled pulses than for those in the pellet fuelled pulses. Although the amplitude $(\Delta\bar{n}_e/\bar{n}_e)$ of the pellet-triggered ELMs is about half that of the natural ELMs, the resulting sputtered fluences are similar. Note that, while the outer strike point is obscured from view, the spectrometer can detect emission from the interaction of the extended ELM filaments with the outer vertical target from where most of the ELM sputtered influx probably originates. Note that the ionisations/photon (S/XB) for these Be and W lines increases with both n_e and T_e, as does the fraction of W^+ ions promptly redeposited at the surface. Without T_e and n_e data of sufficient temporal and spatial resolution it is impossible to evaluate absolute influxes.

Fuelling	**ELM type**	$\Delta n_e/n_e$	$\Delta n_Z/n_Z$ [%]		Φ_{Be}	Φ_W	ζ_{NC} ($dt_{ELM} \leq 20$ ms)	
		ELM [%]	ELM	Inter-ELM	[-]	[-]	Pedestal	Mantle
Gas only	**Natural**	-3.5 ± 0.1	-5.8 ±0.4	6.5 ± 0.6	0.26 ± 0.01	0.16 ± 0.01	-41 ± 8	5.2 ± 0.2
Pellet & Gas	**Natural**	-3.8 ± 0.2	-1.3 ±0.2	1.1 ± 0.3	0.14 ± 0.01	0.10 ± 0.01	-32 ± 8	3.1 ± 0.3
	Pellet	-1.7 ± 0.2	-1.0 ±0.3	3.5 ± 0.6	0.16 ± 0.01	0.12 ± 0.01	-24 ± 7	5.4 ± 0.6
	All	-3.2 ± 0.1	-1.6 ±0.2	3.7 ±0.3	0.19 ± 0.01	0.13 ± 0.01	-34 ± 5	4.5 ± 0.2

Table 1 Average values of data shown in Fig. 4 by fuelling source and ELM type for high-power, 3 MA pulses #92432,3,4&6. Colour highlights significantly lower ■ or higher values ■ than the average over all ELMs.

This work has been carried out within the framework of the EUROfusion Consortium and has received funding from the Euratom research and training programme 2014-2018 and 2019-2020 under grant agreement No 633053 and from the RCUK Energy Programme [grant number EP/P012450/1]. The views and opinions expressed herein do not necessarily reflect those of the European Commission.

[1] Garzotti L. et al., IAEA FEC '18; [2] Giroud C. et al., Nucl. Fusion **53** (2013) 113025;
[3] Field, A. R. et al., EPS 2018; [4] Hatch D. et al., Nucl. Fusion **57** (2017) 036020;
[5] Maggi C. et al., Nucl. Fusion **55** (2015) 113031; [6] Fedorczak, N. et al., JNM 463 (2015) 85-90;
[7] Angioni, C. et al., Phys. Plasmas 22 (2015) 055902; [8] Kim H-T et al., Nucl. Fusion **58** (2018) 036020.